אוניברסיטת בן-גוריון בנגב
Ben-Gurion University of the Negev

Quadrupolar Perturbed NMR in Inorganic Nanomaterials

Alexander M. Panich

Department of Physics, Ben-Gurion University of the Negev, Be'er Sheva, Israel

3rd Joint HFI/NQI International Conference, September 13-17, 2010, CERN, Switzerland

Why inorganic nanomaterials?

A lot of investigations of carbon nanostructures. Their properties have been studied in detail.

In contrast, our knowledge of the physical properties of inorganic nanotubes and fullerene-like species is still limited.

Eventual applications in electronics, magnetic recording, as nano-bio materials, are used as low-friction materials.

NMR is an excellent tool in studying the local structure, electronic structure and chemical bonding in inorganic nanoparticles.

Inorganic nanoparticles often contain atoms with quadrupolar nuclei, such as ^{11}B, ^{14}N, ^{51}V, $^{95,97}Mo$, etc. that nicely suit the topics of the HFI/NQI Conference.

Carbon nanotubes and fullerenes

Graphite and graphene are semimetals. Solid C_{60} is a semiconductor. Properties of carbon nanotube (CNT) vary from metallic to semiconductor behavior depending on wrapping angle.

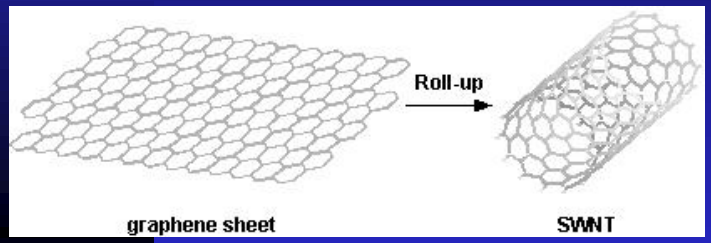

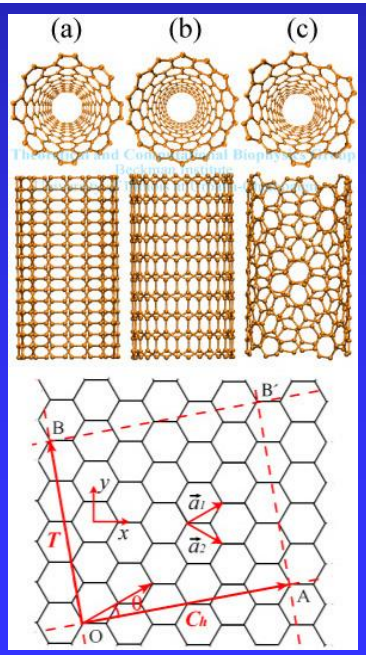

Solid C_{60} is a semiconductor with energy gap 1.5–1.9 eV.

Inorganic nanotubes

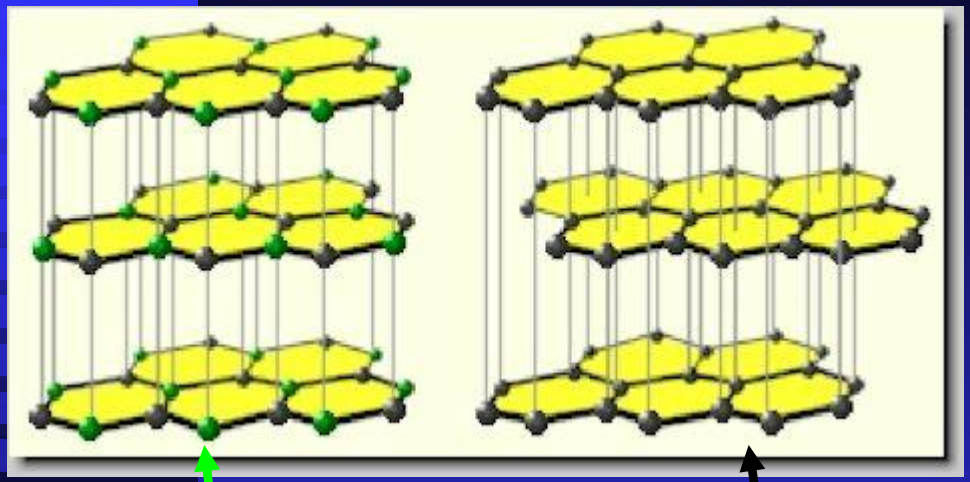

Crystal lattice of
hexagonal boron nitride (left)
and graphite (right)

Similar to CNTs, layered inorganic compounds, such as BN, MoS_2, etc. can also form fullerene-like and tubular nanostructures.

However, they do not show such variation of physical properties as CNTs do. Similar to bulk samples, BNNTs are semiconductors with a wide energy gap 5.5 eV irrespective of diameter and chirality. Boron nitride fullerenes are wide-gap semiconductors as well. MoS_2 fullerenes seem to hold the properties of bulk MoS_2.

Why?

NMR study of electronic properties of inorganic nanomaterials.

Outline

NMR investigation of

- boron nitride nanotubes,

- molybdenum sulfide fullerenes,

- dithallium selenide nanorods

- vanadium oxide nanotubes

- Comparison of the data for bulk and nano-sized samples helps to understand properties of the nano-sized compounds.

Boron nitride nanotubes

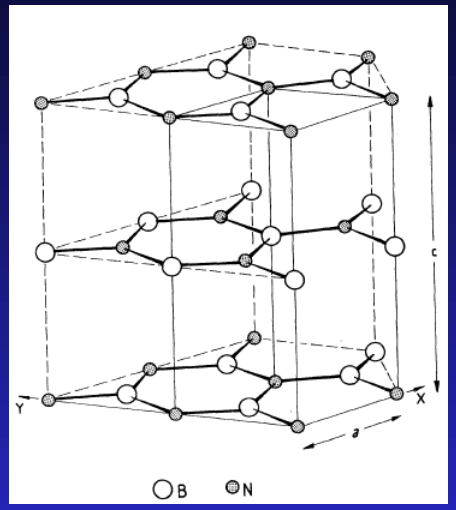

Crystal lattice of hexagonal boron nitride

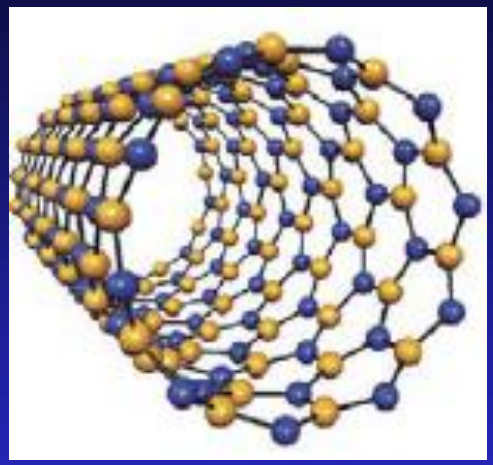

Tubular BN

First NMR study of BNNTs

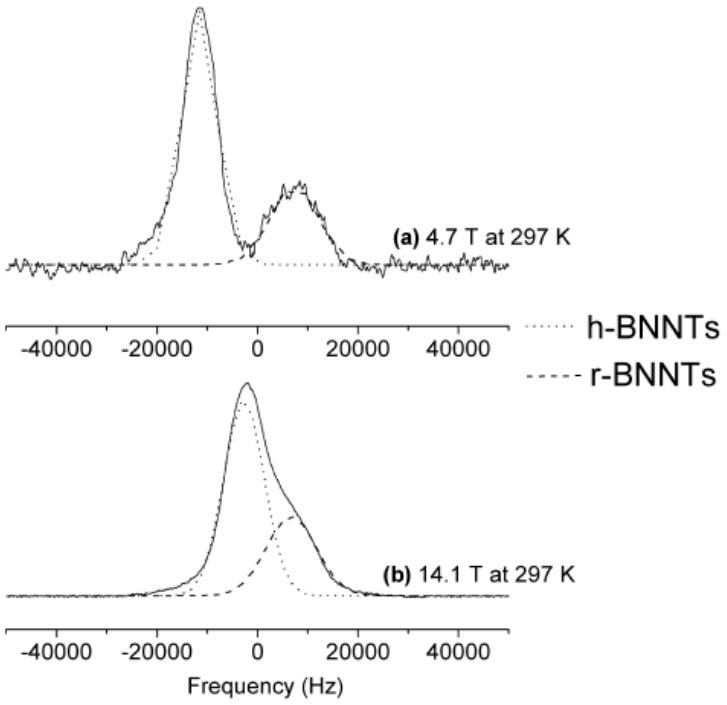

^{11}B NMR spectra of BNNTs in magnetic fields of 4.7 T and 14.1 T (Jung et al, Solid State Commun., 2004).

Interpretation of ^{11}B NMR spectrum: two components arising from BNNTs with different structures (hexagonal and rhombohedral phases) showing different chemical shift.

But! But! If so, splitting should increase with increasing magnetic field.

In experiment - just in opposite!

Quadrupole splitting?

Our study of multi-wall boron nitride nanotubes

SEM and TEM images of our multiwall BN nanotubes.

Averaged inner diameter ~ 7 nm, length about 1–2 μm, ~20 walls.

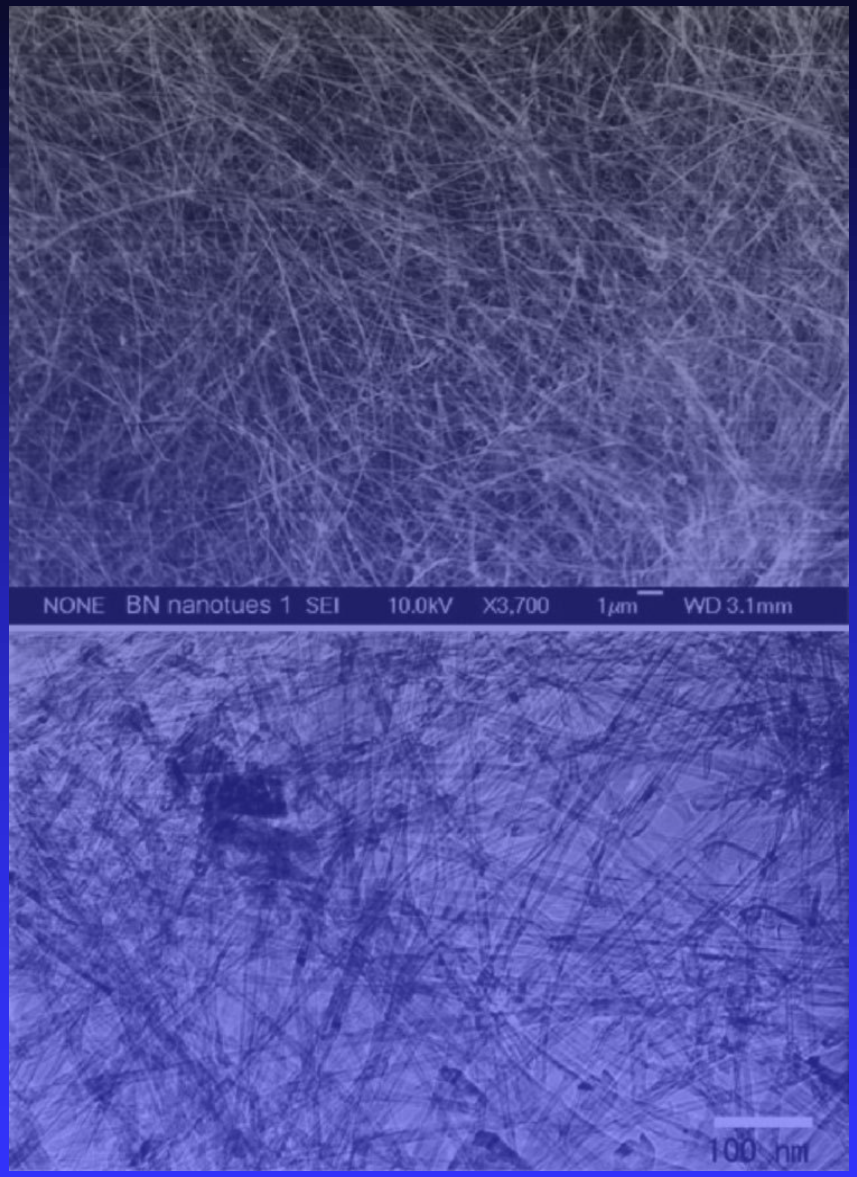

Our NMR study of BNNTs

^{11}B (I=3/2) – quadrupole nucleus

$$H = -\gamma_n \hbar B_0 I_z + \frac{e^2 qQ}{4I(2I-1)}(3I_z^2 - I^2) + H_{dip} + H_{cs}$$

$H_z >> H_Q$- the quadrupole interaction is a perturbation to the Zeeman term.

I = 3 /2 - the NMR spectrum consists of 3 transitions.

Central 1/2→−1/2 transition is not affected by the first order effects and is observed at the Larmor frequency,

Satellites 3/2→1/2 and −1/2→−3/2 are shifted to frequencies determined by the product ν_Q $(3\cos^2\theta\text{-}1)/2$, where $\nu_Q = e^2qQ/2h$. In a powder, the satellite lines are distributed over the frequency range of the order of $2\nu_Q$ with the singularities at $\pm\nu_Q/2$ and shoulders at $\pm\ \nu_Q$ and are hardly detected.

H_{dip} ,H_{CS} << H_Q; CSA(^{11}B) ~ 27-40 ppm in *h*-BN and BNNTs

Room temperature ^{11}B NMR spectrum

(A. M. Panich et al., Phys. Rev. B, 2006)

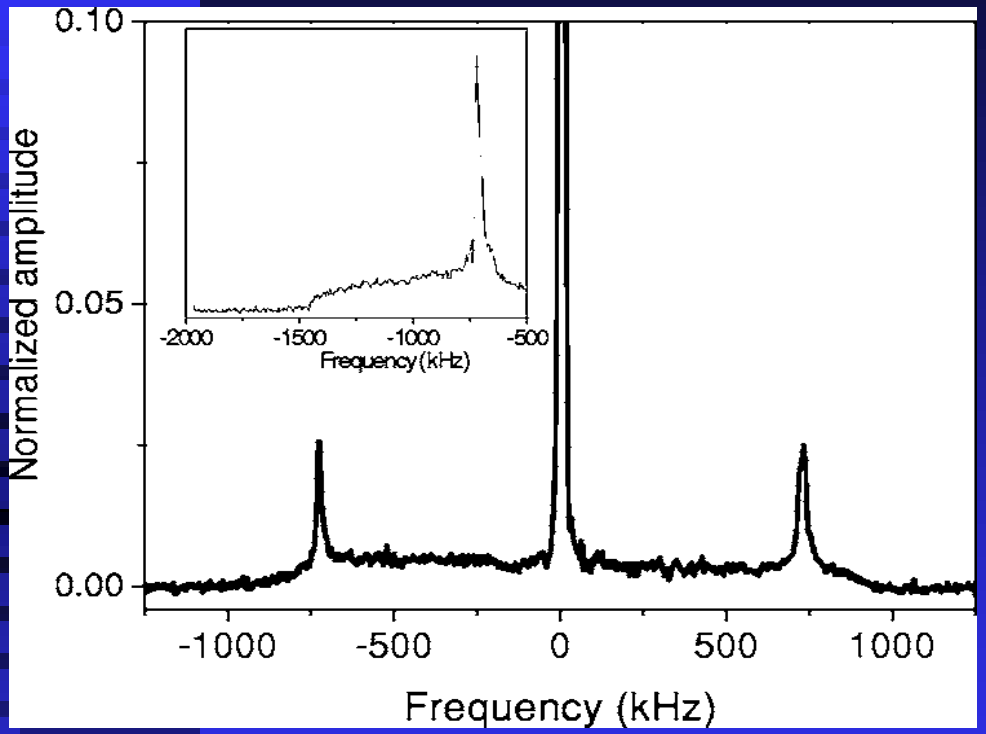

Room temperature ^{11}B NMR spectrum in magnetic field B_0=8.0196 T. In inset, separately measured low-frequency satellite is shown.

Room-temperature experimental ^{11}B NMR spectrum.

From the splitting between satellites, $\Delta=\nu_Q = e^2qQ/2h$ the values of ν_Q = 1.453 MHz and quadrupole coupling constant e^2qQ/h = 2.906 MHz were found.

Neither a splitting nor any unexpected broadening of the satellite transitions was observed, leading to the conclusion of a zero value of the asymmetry parameter η.

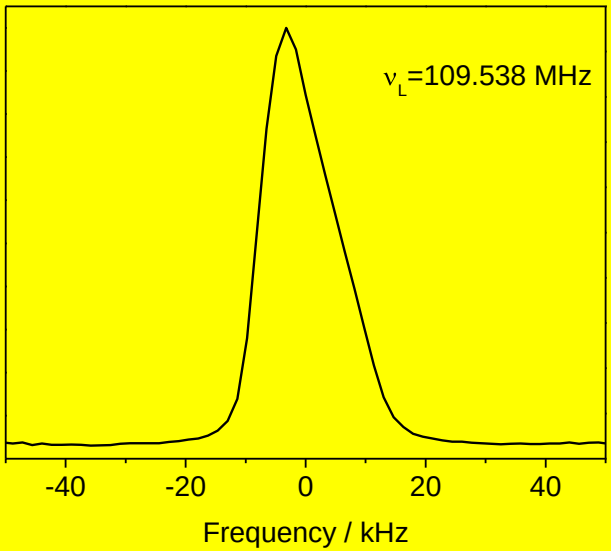

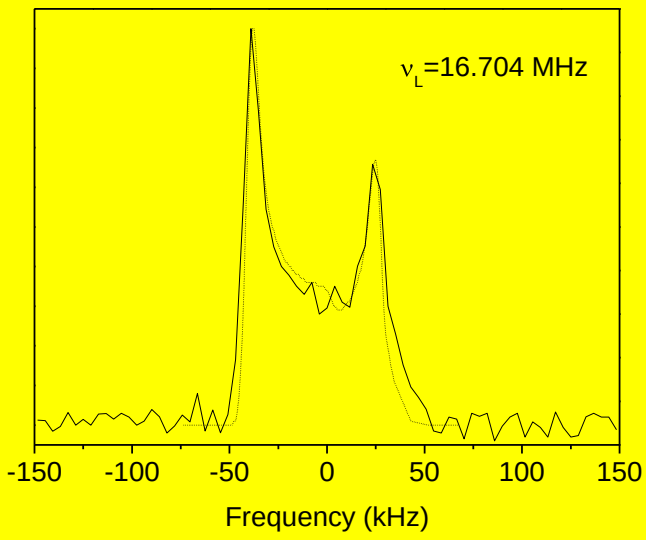

Central (1/2→-1/2) transition

The shape of the central transition is determined by the second-order quadrupolar effects. For I=3/2, line shape in powder sample exhibits two singularities with splitting

$$\Delta = 25\nu_Q^2/48\nu_0$$

The separation between two peaks, observed at ν_0=16.7 MHz, is 63.5 kHz, yielding ν_Q=1.427 MHz and e^2qQ/h=2.854 MHz.

No doubts - quadrupolar splitting.

Temperature dependence of ν_Q

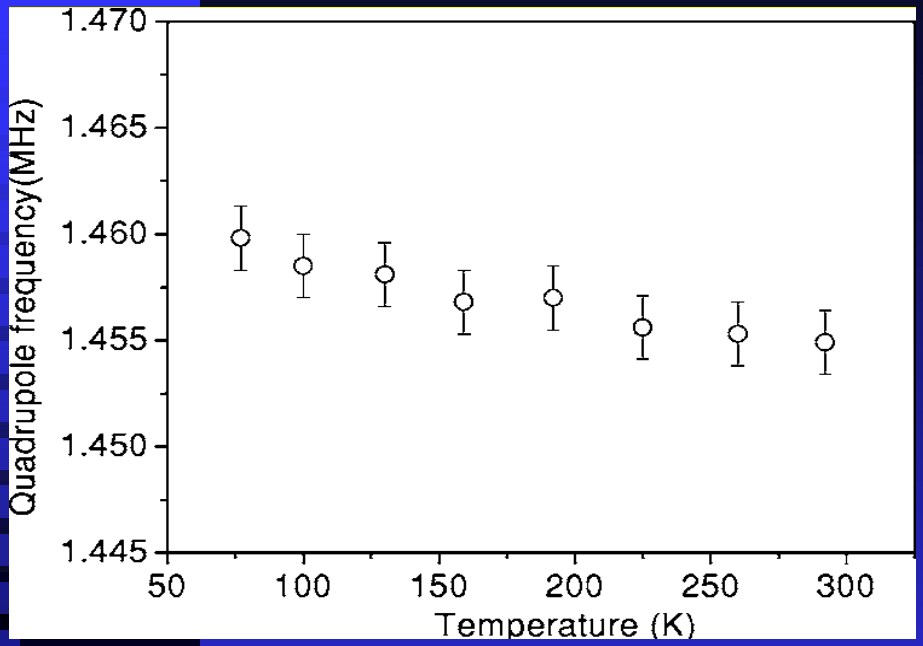

Temperature dependence of the quadrupole Frequency in BNNTs.

Increase in ν_Q with decreasing temperature is mainly caused by freezing of the low-frequency torsional librations of a molecule as a whole that are large for molecular crystals but are small for the bulk *h*-BN and long multiwall BNNTs.

Therefore the lattice dynamics of BN are mainly due to zero-point vibrations.

The quadrupole frequency in *h*-BN, measured at 4.2 K by SQUID, was found to be 1.467 kHz – close to that RT that confirms weak temperature dependence of ν_Q in *h*-BN.

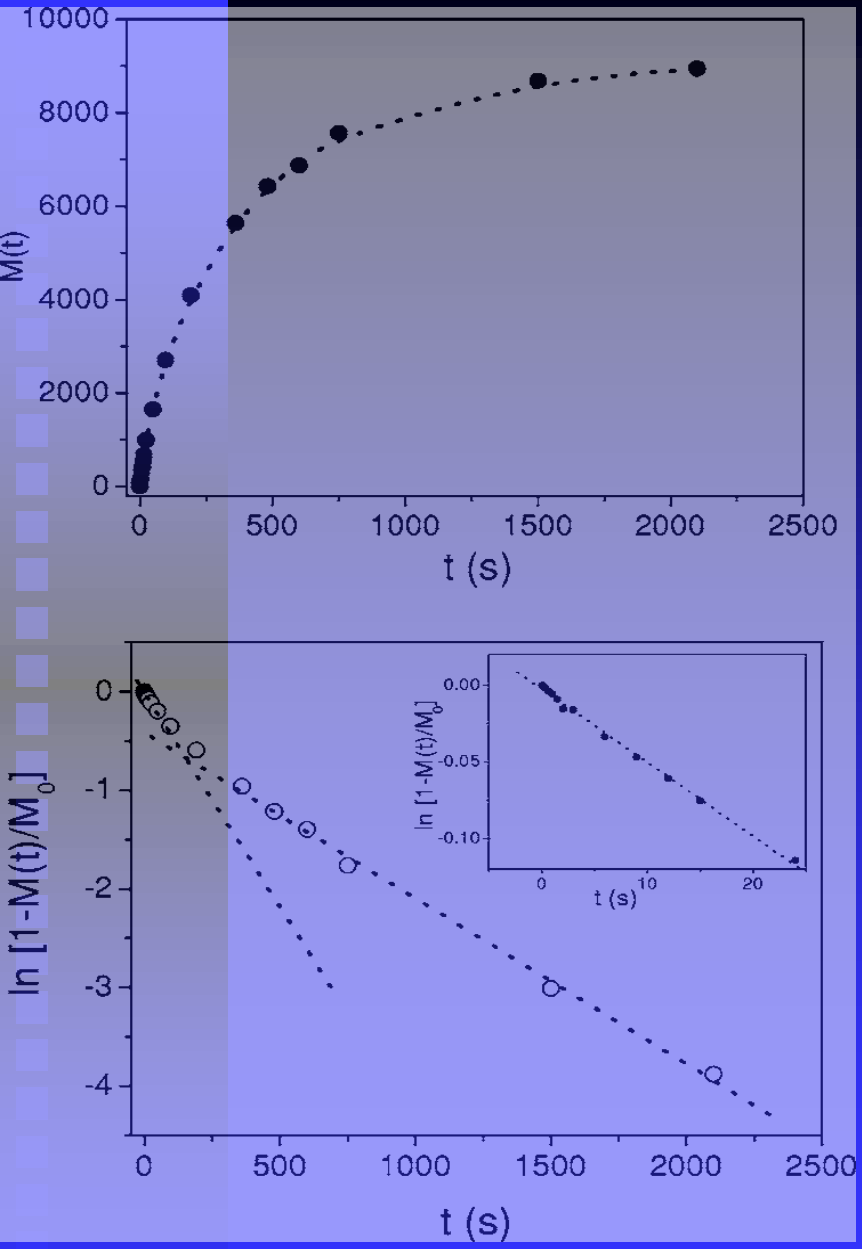

Spin-lattice relaxation measurement (ν_0=109.58 MHz)

^{11}B magnetization recovery in the linear and semi-logarithmic scales may be fit as a superposition of two exponentials with very long ^{11}B spin-lattice relaxation times

T_{11}= 76 ± 13 s, and T_{12} = 495 ± 21 s.

How to explain?

EPR

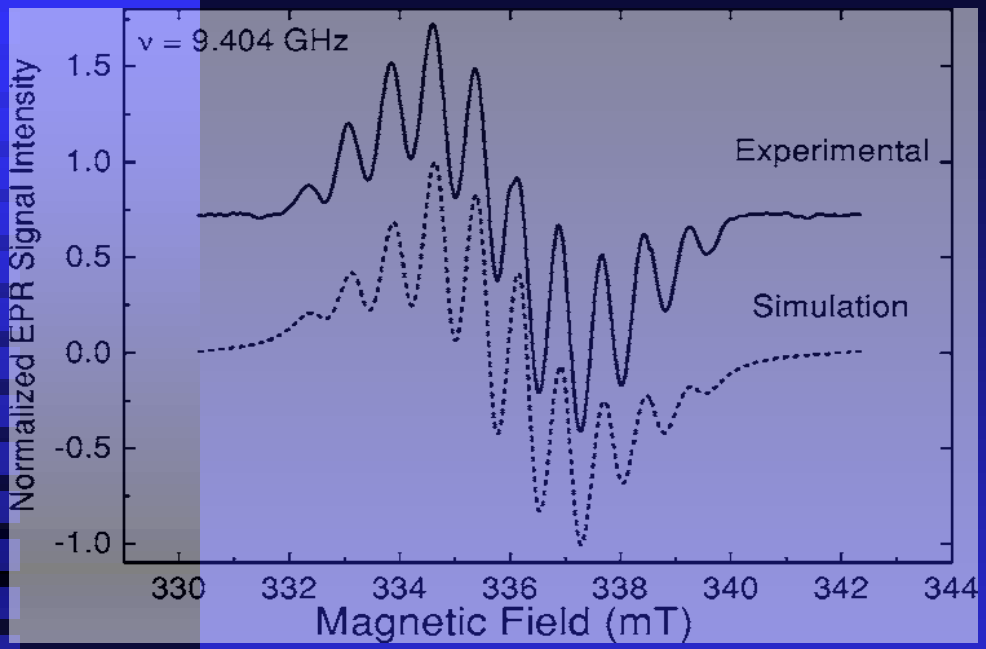

EPR signal: 10 well-resolved lines due to unpaired electron trapped in a nitrogen vacancy, which is surrounded by m=3 equivalent boron atoms.

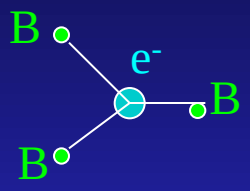

Number of hyperfine components is
$N = 2\ I\ \ m + 1 = 10$,
where $I(^{11}\mathrm{B})=3/2$.

Density of PM centers determined by EPR, 9 10^{15} spin/g, is less than the estimated number of the nanotubes in our sample, thus there are nanotubes either with or without paramagnetic centers.

Two exponentials may correspond to NTs with and without paramagnetic centers.

Quadrupole coupling constants of bulk *h*-BN and BN nanotubes at ambient temperature

Compound	e^2qQ/h, MHz	Reference
Bulk *h*-BN	2.96 ± 0.10	[25]
Bulk *h*-BN	2.9	[26]
Bulk *h*-BN	3.00 ± 0.10	[23]
Bulk *h*-BN	2.936 ± 0.020	[27]
Bulk *h*-BN	3.2	[28]
BN nanotubes	2.880 ±0.026	Our data

23. M. Fanciulli, M. Corti, Phys. Rev. B **52**, 11872 (1995).
25. A. H. Silver, P. J. Bray, J. Chem. Phys. **32**, 288 (1960).
26. P.S. Marchetti, D. Kwon, W.R. Schmidt, L.V. Interrante, G.E. Maciel, Chem. Mater. **3**, 482 (1991).
27. G. Jeschke, W. Hoffbauer, M. Jansen, Solid State Nucl. Magn. Reson. **12**, 1 (1998).
28. K. Kanehashi, K. Saito, J. Molec. Struct. 602-603, 105 (2002).

Discussion

Closeness of QCC of the MW BNNTs and bulk *h*-BN reflects:

similar chemical bonding,
similar charge distribution over B-N bond,
and similar local symmetry.

These findings should result in similar electronic properties.

That is why BN nanotubes are semiconductors with a nearly constant energy gap of 5.5 eV regardless of diameter, chirality, number of walls of the tube, and this gap is close to that of bulk *h*-BN (experiment: ~5.8 eV, calculations: 5.4-5.5 eV).

Discussion (continued)

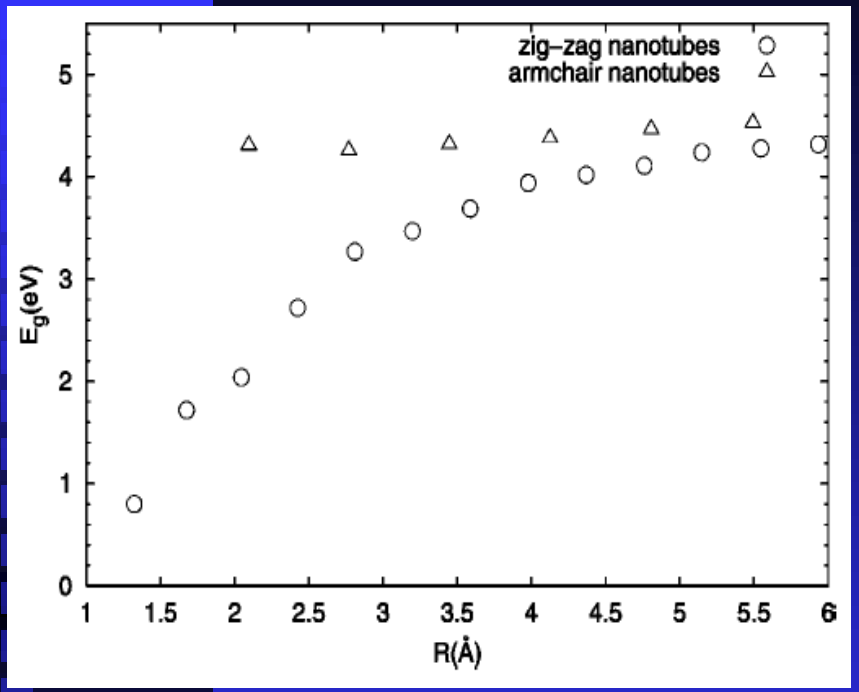

Energy gaps of BN nanotubes vs radius
(H.J. Xiang et al, Phys. Rev. B, 2003)

Perhaps only BNNTs with very small diameter would show different electronic properties with respect to those of bulk *h*-BN and a decrease of the band gap caused by the curvature of the sheets and appearance of some $sp^2 \rightarrow sp^3$ re-hybridization.

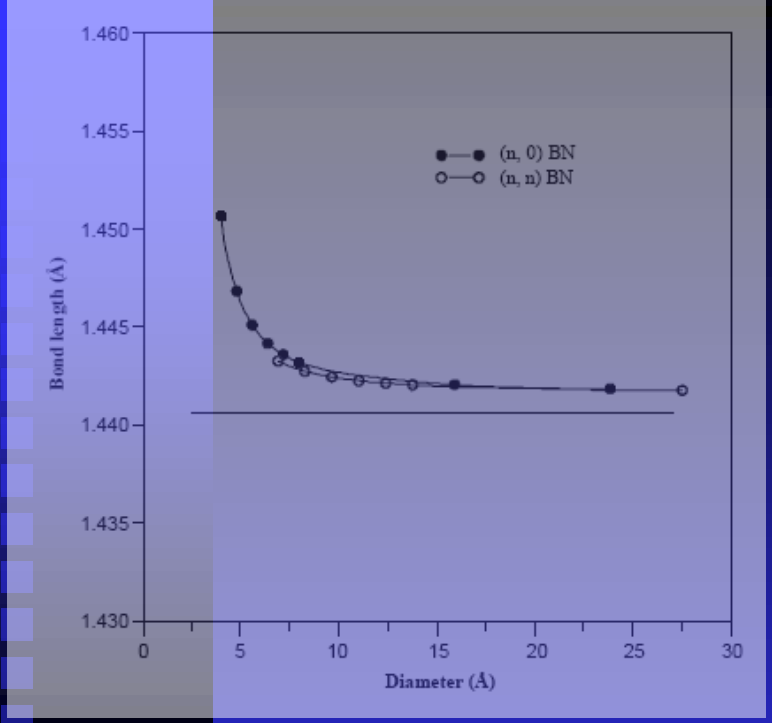

Bond length of the BN nanotubes as a function of diameter. Solid line - bond length of h-BN. (Moon et al, Physica E, 2004)

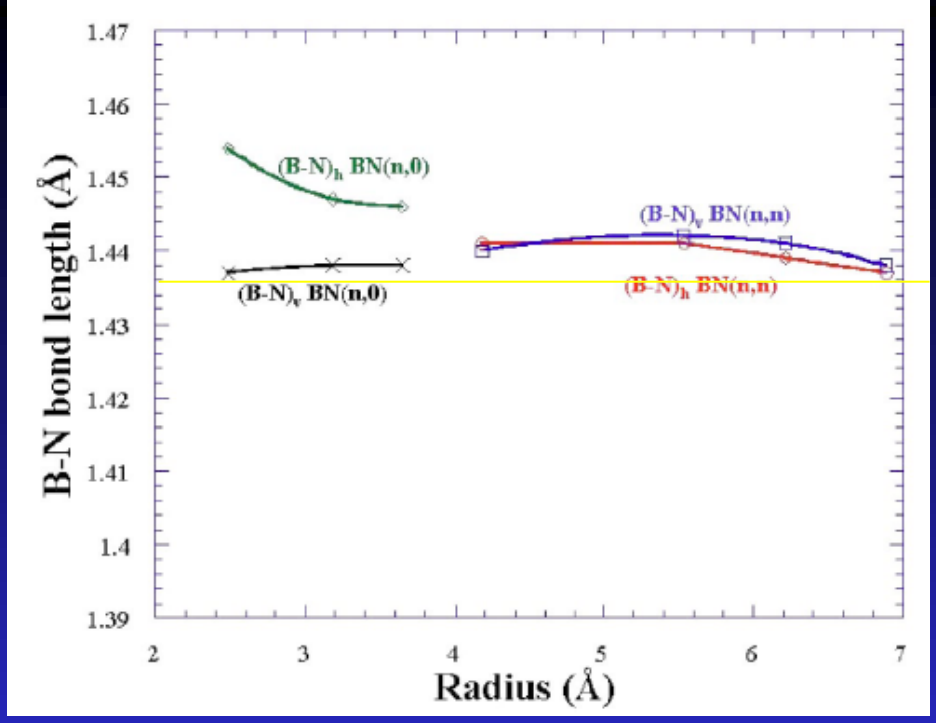

Bond lengths of BN-NT's as a function of tube radius. Yellow line - bond length in h-BN, 1.446 Å (Akdim et al, Phys. Rev. B, 2003).

Calculations: B-N bond length in nanotubes is 1.438 Å, almost equal to the experimental value in bulk *h*-BN 1.446 Å. Very small variations in the bond length with tube radius, except for BNNTs with very small diameter.

Our BNNTs: average inner diameter ~ 7 nm, length about 1–2 mm, ~ 20 walls ranging from 8 to 40 layers.

Inorganic Fullerenes (IF) MoS_2

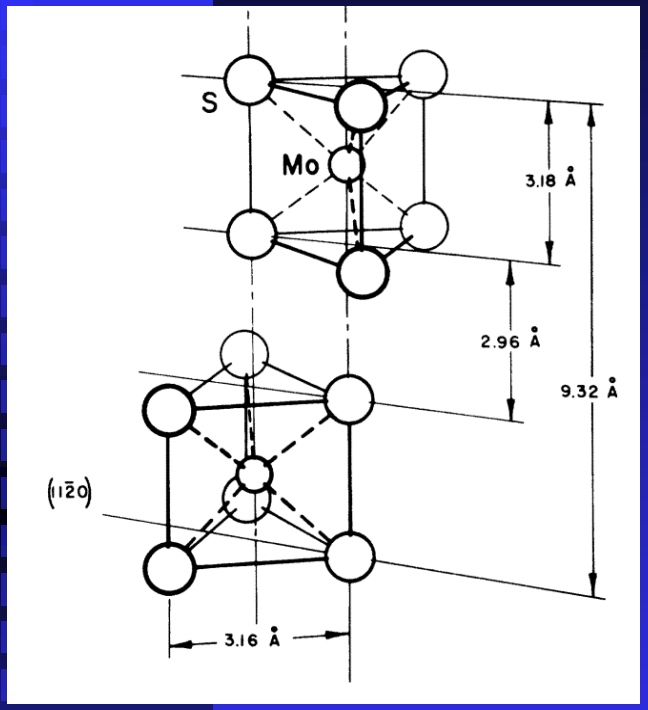

2H-MoS_2: triple S–Mo–S layers bound by van der Waals forces

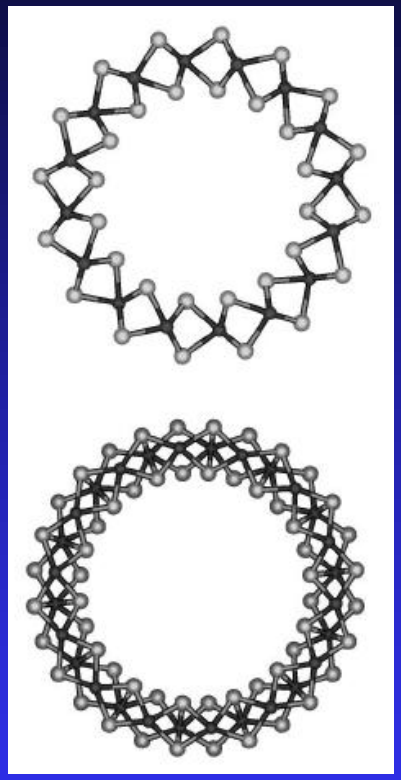

Armchair (top) and zigzag (bottom) MoS_2 nanotube (Seifert et al., PRL, 2000)

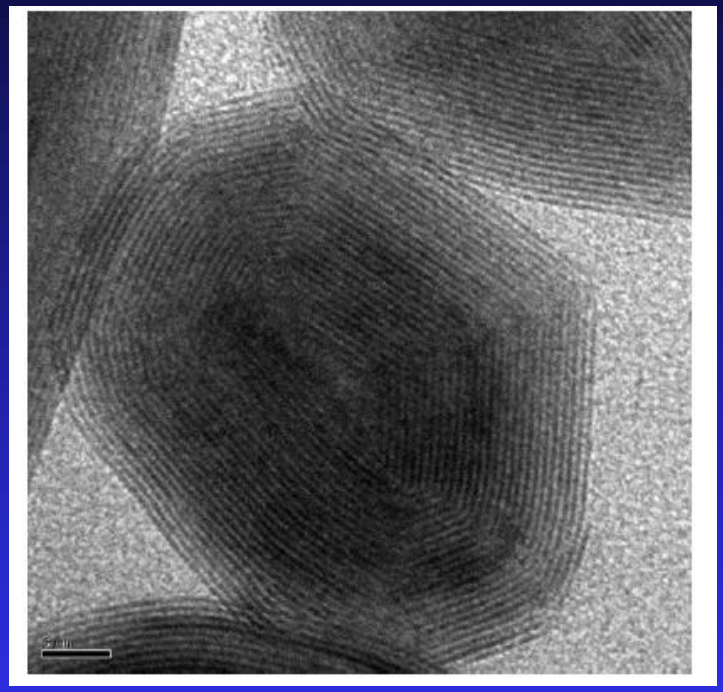

TEM image of IF-MoS_2 particle.

A polyhedral onion-like structure, size ~ 40 nm, 20–30 MoS_2 layers, interlayer distance of 0.62 nm as in bulk 2H-MoS_2.

First ^{95}Mo NMR study of IF-MoS_2 and, for comparison, of bulk 2H-MoS_2 sample

(Panich et al, J. Phys. Condensed Matter, 2009)

^{95}Mo (15.7%) and ^{97}Mo (9.5%), $I = 5/2$ – quadrupole nuclei.
Low natural abundance,
low resonance frequency (22.2 MHz in $B_0 = 8$ T),
broad spectra due to quadrupole coupling and
very long spin–lattice relaxation time in nonmetallic specimens,
make measurements of Mo NMR spectra in powders difficult.

Only a few Mo NMR measurements in solids, some of them - using ^{95}Mo enriched samples.

T.G. Bastow: ^{95}Mo NMR of bulk 2H-MoS_2 with natural abundance of the ^{95}Mo. Was in two minds, whether line shape is caused by second-order quadrupole interaction, by chemical shielding anisotropy, or by both these effects.

For the axially symmetric electric field gradient ($\eta = 0$) caused by the axial (threefold) symmetry of the Mo site, the second order shift of the central component is

$$\nu(\frac{1}{2} \leftrightarrow -\frac{1}{2}) = -(\frac{\nu_Q^2}{16\nu_0})[I(I+1) - \frac{3}{4}](1-\mu^2)(9\mu^2 - 1)$$

$\mu = \cos\theta$, where θ is the angle between the principal axis of the electric field gradient and the applied magnetic field, and ν_0 is the Larmor frequency.

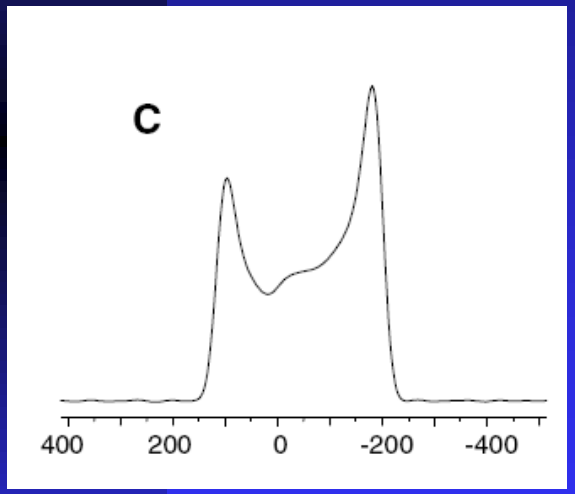

Spacing between the two peaks is

$$\Delta = \nu_1 - \nu_2 = \frac{25\nu_Q^2}{144\nu_0}[I(I+1) - \frac{3}{4}]$$

For I =5/2 $\nu_Q = \frac{3}{20}(\frac{e^2qQ}{h})$

$$\Delta = \frac{25\nu_Q^2}{18\nu_0}$$

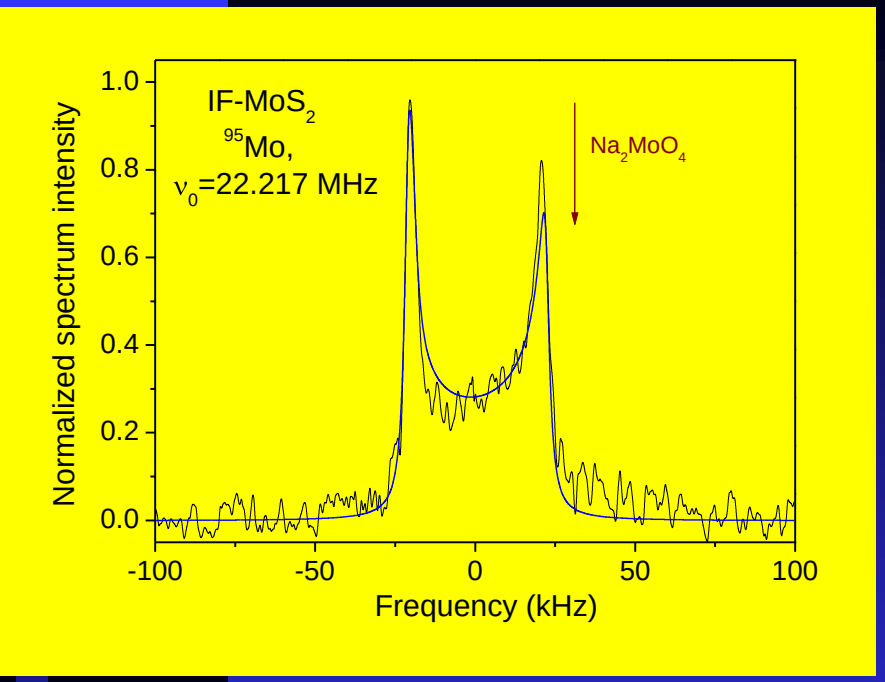

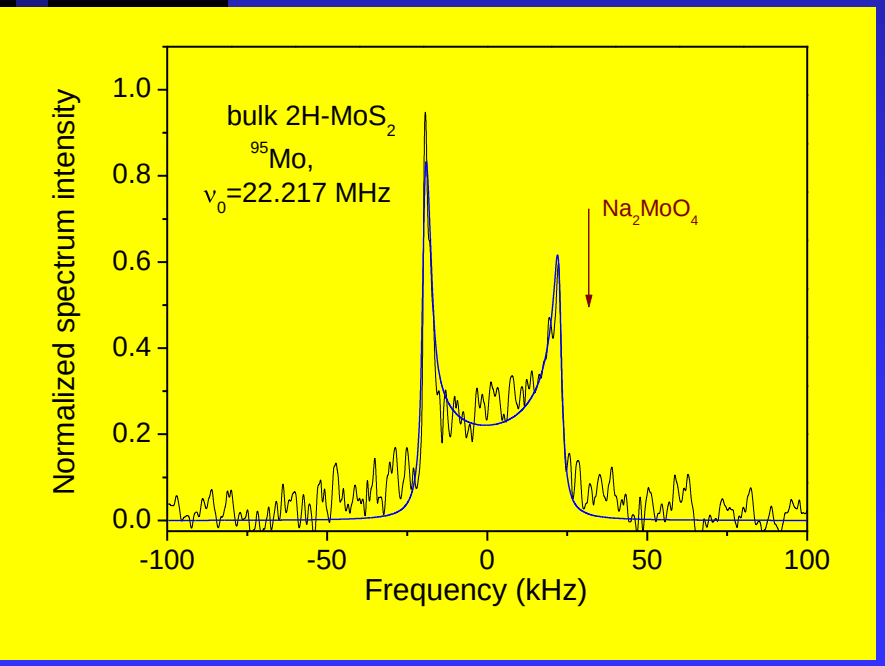

Experimental room temperature ^{95}Mo NMR spectra of bulk 2H-MoS2 (bottom) and IF-MoS2 (top) samples and the simulated spectra (blue lines).

Our measurements in $B_0 = 8$ T reveal nearly the same splitting $\Delta = 41.2$ and 41.6 kHz for IF and bulk samples, respectively.

Bastow, bulk 2H-MoS_2, 9.4 T, 26.06 MHz : $\Delta = 42.7$ kHz. Since quadrupolar splitting $\Delta \sim 1/\nu_0$, smaller $\Delta \sim 35$ kHz is expected.

The only way to reconcile our data with those of Bastow is to take into account a contribution of chemical shielding anisotropy to the NMR line shape for powder samples, which may be essential for heavy nuclei such as ^{95}Mo.

For the axially symmetric shielding tensor, this contribution is described by the expression

$$\nu = \nu_0[1+\alpha(3\mu^2-1)]$$

Combined nuclear quadrupole and anisotropic chemical shift effects in a single crystal result in the following expression for the central transition

$$\nu(\frac{1}{2}\leftrightarrow-\frac{1}{2}) = \nu_0\{1+(\frac{\nu_Q^2}{16\nu_0})[I(I+1)-\frac{3}{4}](1-\mu^2)(9\mu^2-1)+\alpha(3\mu^2-1)\}$$

In a powder, the line shape possesses two singularities and a step, with splitting between the maxima

$$\Delta = \nu_2-\nu_1 = \frac{25b}{9\nu_0}-\frac{5}{3}\alpha\nu_0+\frac{\alpha^2\nu_0^3}{4b} = \frac{25\nu_Q^2}{18\nu_0}-\frac{5}{3}\alpha\nu_0+\frac{\alpha^2\nu_0^3}{2\nu_Q^2}$$

$$b = \frac{\nu_Q^2}{16}[I(I+1)-\frac{3}{4}]$$

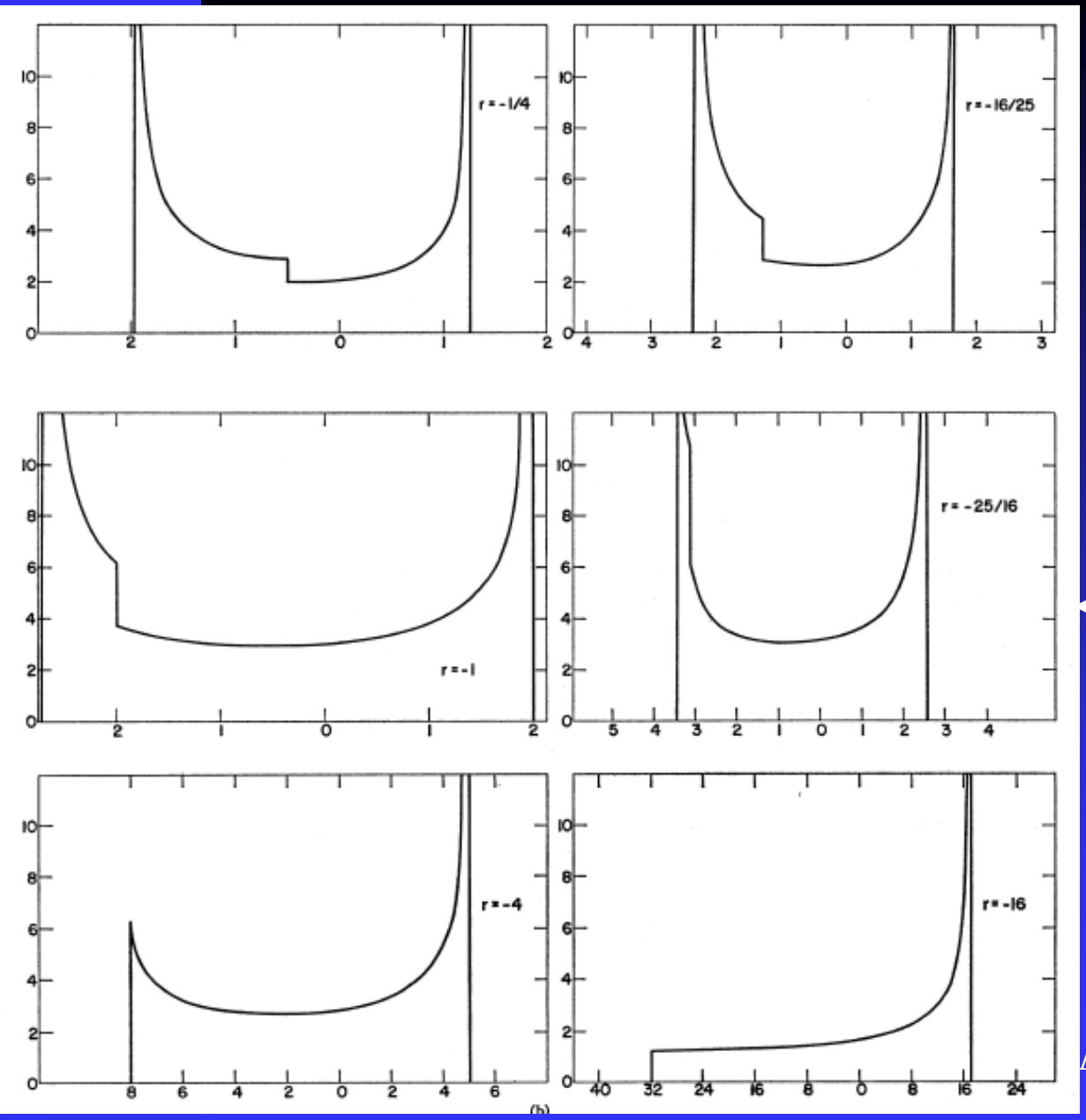

$$r = \frac{\alpha \nu_0^2}{b}$$

$$\alpha = \frac{\sigma_{//} - \sigma_{\perp}}{3}$$

← our case

Abscissa, $(\nu-\nu_0)$, in units $\frac{b}{\nu_0} = \frac{\nu_Q^2}{2\nu_0}$

Jones W.H., Graham T.P. and Barnes R.G., *Phys. Rev.* **132** 1898 (1963)

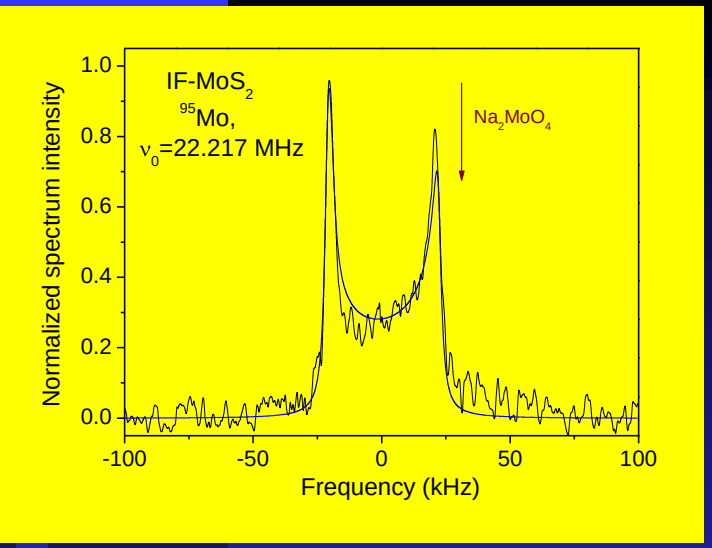

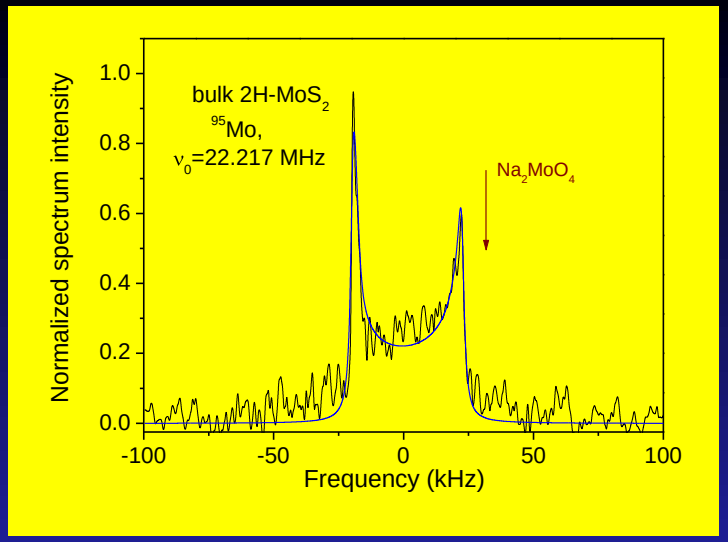

^{95}Mo spectra simulation using DMfit2009 software (D. Massiot et al., *Magn. Reson. Chem.* **40** 70 (2002)).

r~-1.47

Compound	ν_Q, kHz	$\frac{e^2qQ}{h}$, MHz	$\Delta\sigma = (\sigma_{//} - \sigma_{\perp})$, kHz	$\Delta\sigma = (\sigma_{//} - \sigma_{\perp})$, ppm
MoS_2 nano	578 15	3.85 0.1	- 33.53	- 1510 80
MoS_2 bulk	565 25	3.77 0.16	- 32.6	- 1470 100

NMR parameters for bulk and nanoparticles are close to each other.

Discussion

1. MoS_2 nanoparticles exhibit QCC and CSA similar to that in bulk compound, reflecting similar local crystal structure, local symmetry, chemical bonding, and charge distribution over the Mo–S bond in bulk and IF samples. This fact results in similar electronic properties of these materials.

It seems that Mo–S bonds are strong enough to hold Mo–S and Mo–Mo distances and are little affected by weak curvature of the layers. Perhaps only single-wall IFs with very small diameter and large curvature would show different electronic properties compared to those of bulk. Multiwall –> close to bulk.

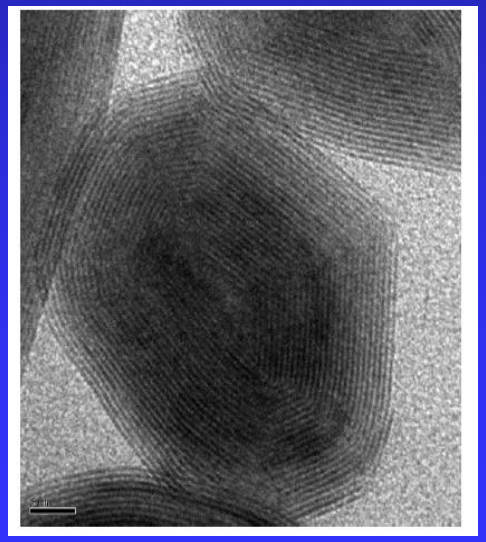

Is there any difference between bulk and nano?

^{95}Mo Spin–lattice relaxation measurements:

very long spin–lattice relaxation times T_1 ~ 255 s and 122 s for bulk MoS_2 and IF-MoS_2, respectively. Reduced T_1 in IF-MoS_2 compared with that in bulk sample is attributed to larger density of paramagnetic defects and to interaction of nuclear spins with electron spins of these defects, which gives rise to effective spin-lattice relaxation channel. This is confirmed by

EPR measurements: $N = 1.9 \times 10^{16}$ spin/g for bulk 2H-MoS_2
and $N = 1.16 \times 10^{17}$ spin/g for IF-MoS_2.

MoS_2-IF have more defective structure than the bulk sample.

Nearly defect-free MoS_2 flat faces with a limited number of defects at the edges of polyhedral nanoparticles appearing upon folding of the triple MoS_2 sheets, when some atoms are left unbound and form defects with dangling bonds. Such defects arise from the difficulty in formation a perfect polyhedral structure by the folding of triple MoS_2 layers.

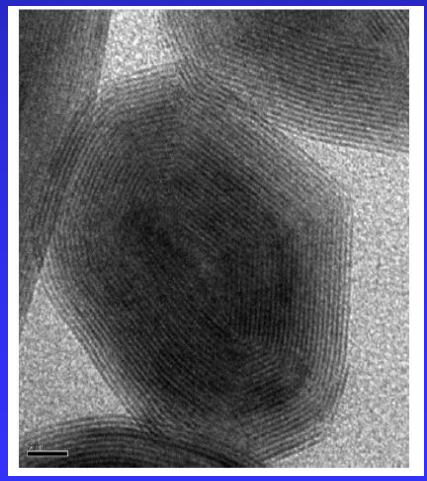

Attempt to observe an NMR signal from the ^{97}Mo isotope

Since the quadrupole moment eQ of ^{97}Mo is 11.5 times larger than that of ^{95}Mo and since the relaxation time T_1 is proportional to $(eQ)^{-2}$, one can expect a much shorter T_1 for ^{97}Mo which could be of a great advantage in the present experiments.

However, the linewidth of the central transition caused by second-order quadrupolar interaction varies as $(eQ)^2$ and thus should yield a linewidth of the order of 5.5 MHz.

Therefore the ^{97}Mo NMR signal was not detected.

Conclusion on BNNTs and MoS_2-IFs

Multiwall BN nanotubes and multishell inorganic fullerenes MoS_2 exhibit QCC and CSA similar to those in the bulk compounds, reflecting similar local crystal structure, chemical bonding, and charge distribution over the B-N and Mo–S bonds in bulk and nano-materials.

These findings result in similar electronic properties of the corresponding bulk and nano-materials.

Tl_2Se: properties of inorganic nanomaterial differ from those of bulk samples

Comparative NMR study of bulk and nanorod samples of Tl_2Se

The average size of Tl_2Se nanorods is about 75 nm in diameter and 900 nm in length.

(A. M. Panich, M. Shao, C. L. Teske, W. Bensch, Phys. Rev. B, 2006)

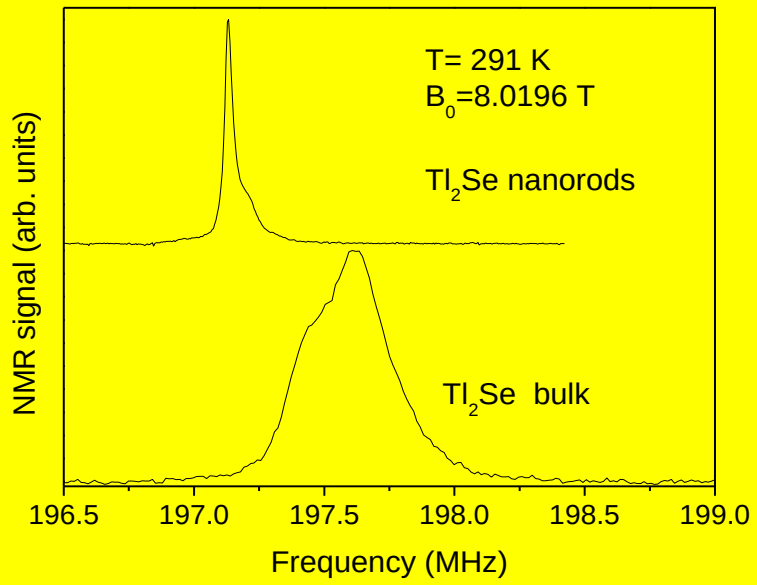

^{205}Tl NMR spectra of bulk and nanorod Tl_2Se samples at T=291 K and B_0=8.0196 T.

Tl_2Se nanorods show a regular chemical shift, bulk Tl_2Se exhibits Knight shift characteristic of conductors, which originates from the hyperfine interaction between nuclear spins and conduction electrons.

$$K = \frac{8\pi}{3} <|\psi(0)|^2>_{E_F} \chi_e^s$$

However, Knight shift in bulk Tl_2Se (0.3%) is much smaller than that in Tl metal (1.6% of the Larmor frequency).
Such value is characteristic of a semimetal showing reduced density of states (DOS) at the Fermi level.

Spin-lattice relaxation: Korringa term in Tl_2Se, $1/T_1T = 1.2\ s^{-1}K^{-1}$, is much smaller than that of Tl metal, $1/T_1T \approx 330\ s^{-1}K^{-1}$, indicating much smaller DOS at the Fermi level of Tl_2Se in comparison with that in metallic thallium; such value is characteristic of semimetals.

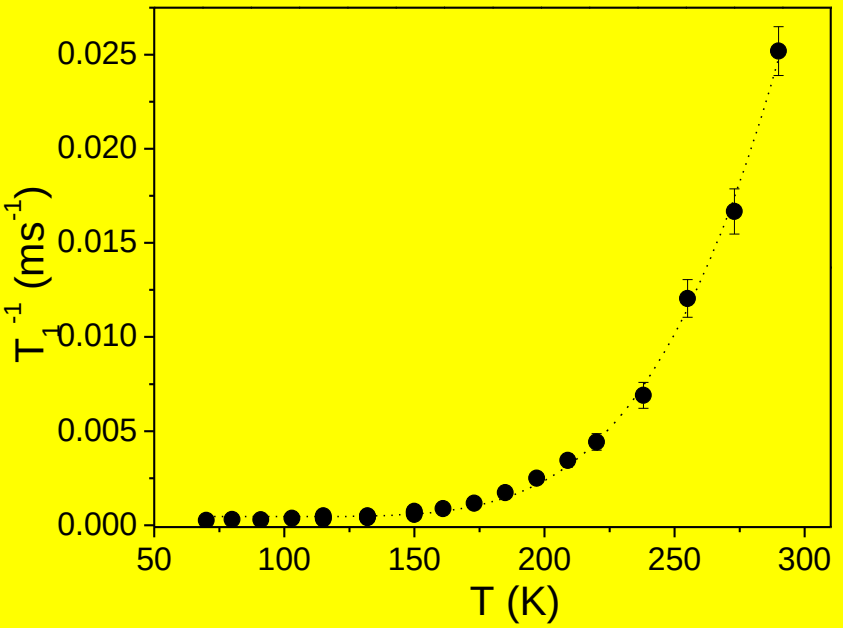

Temperature dependence of ^{205}Tl spin-lattice relaxation rate of Tl_2Se nanorod sample in B_0=8.0196 T. Exponential fit is shown by dotted line.

Tl_2Se nanorods are semiconductors and exhibit a characteristic activation behavior in the spin-lattice relaxation rate due to the thermal excitation of carriers to the conduction band. The activation energy was determined to be ΔE =0.24 eV.

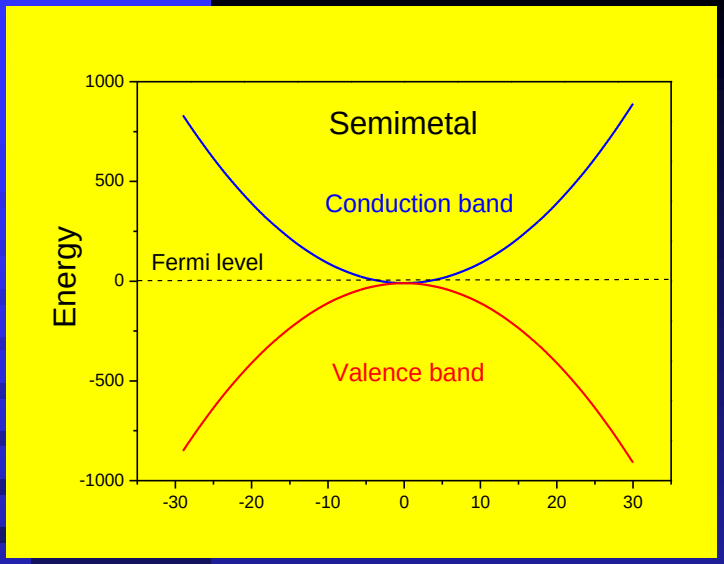

In semimetal conduction and valence bands touch each other. Such band structure is sensitive to different effects, which may cause gap opening. Size reduction can significantly change the properties of the compound.

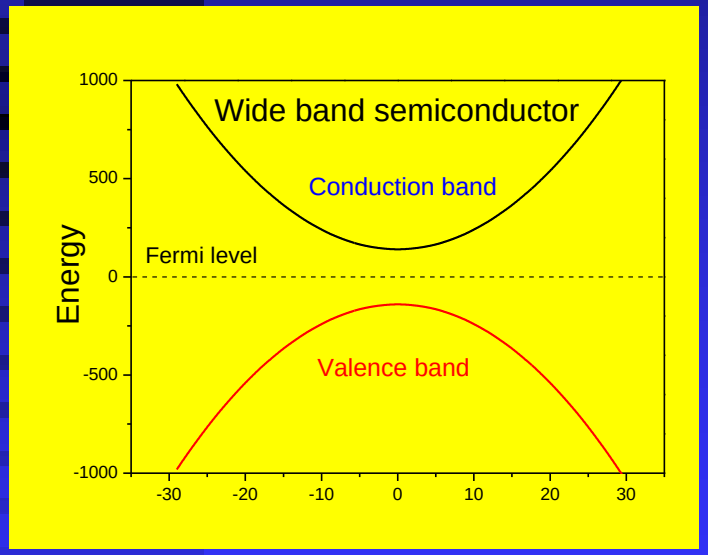

Analogous bulk-to-nano transformation of insulators and wide gap semiconductors does not show visible changes in their properties.

Vanadium oxide nanotubes

Vanadium oxides often crystallize as layered compounds. They may be diamagnetic, paramagnetic, ferromagnetic, show metal-insulator transition, superconductivity, etc. VO_xNTs are of interest due to their application in spintronics, which requires fabrication of magnetic nano-structures.

Structure of VO_xNTs is composed of scrolled V_7O_{16} layers between which alkylamine molecules (acting as the structure-directing agents) are embedded.

They are considered to be of mixed valence containing V^{4+} and V^{5+} ions, which would be seen in the NMR spectra.

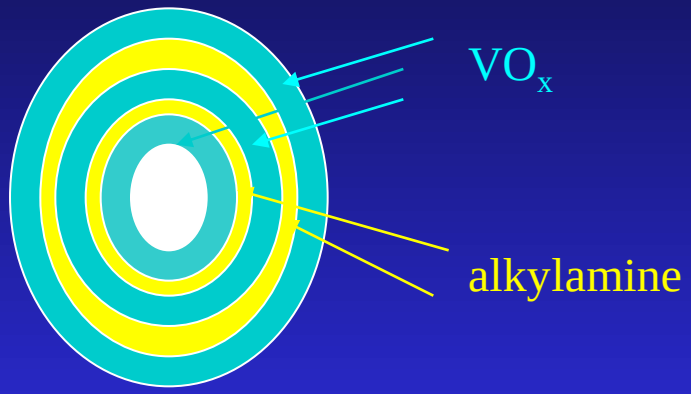

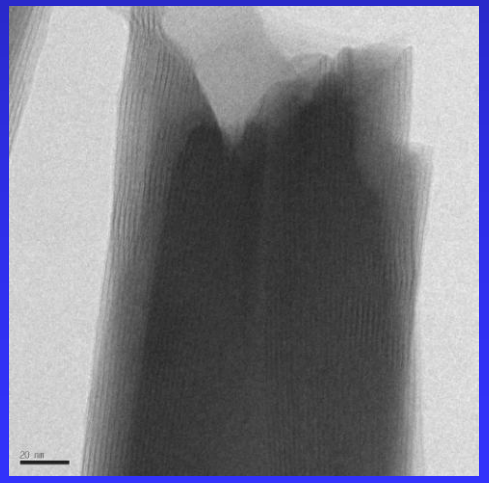

TEM image of the VO_x nanotube

VO_x-decylamine nanotubes $[CH_3(CH_2)_9NH_2]$-VO_xNT or C10-VOxNT

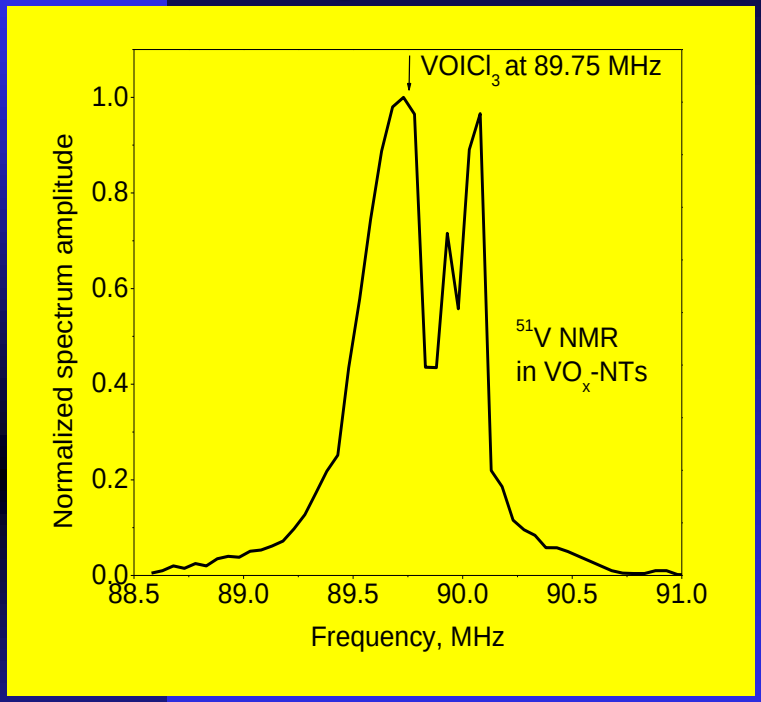

Room temperature ^{51}V NMR spectrum of VO_x nanotubes. Arrow shows position of $VOCl_3$ reference.

^{51}V NMR spectrum: 3 peaks at ~89.73 MHz, ~89.93 MHz and ~90.06 MHz.

Position of the low frequency line is close to that of diamagnetic $VOCl_3$ and is attributed to diamagnetic V^{5+} ions.

High frequency resonances reveal a "paramagnetic" shift of 200 - 300 kHz and are assigned to two inequivalent paramagnetic V^{4+} ions.
The ratio of the intensities $I_d/(I_{p1}+I_{p2}) \sim 2.13$, which yields a rough estimation of 68% of V^{5+} and 32% of V^{4+} ions.

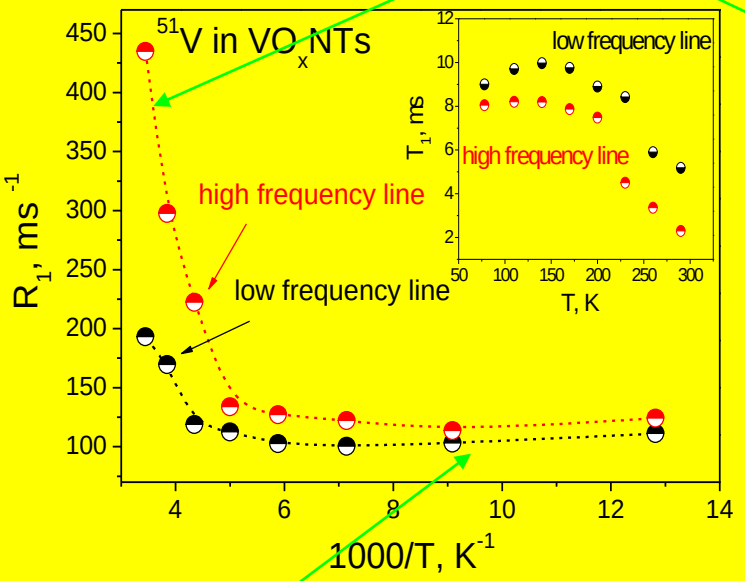

Temperature dependence of ^{51}V spin-lattice relaxation time in VO-NTs

Two main contributions to spin-lattice the relaxation (NSLR):

Quadrupole contribution to NSLR results from modulation of quadrupole interaction by lattice vibrations, yielding temperature dependence

$$R_{1Q} \sim T^2\left(a - \frac{b}{T^2}\right) \quad \text{and} \quad R_{1Q} \sim T^7$$

for low and high temperatures, respectively. Increase in T_1 on cooling in the high temperature region is attributed to the quadrupole contribution to the NSLR.

Magnetic contribution to NSLR due to coupling of nuclear spins with electron spins of the paramagnetic ions

$$R_1^m \sim \frac{\tau_e}{1+\omega_0^2\tau_e^2}$$

ω_0 - NMR frequency, τe - electron correlation time. $\tau_e \sim 10^{-9}$-10^{-12} s, $\omega_0\tau_e \ll 1$ and $R_1 \sim \tau_{e0}\exp(E/k_BT)$

T_1^m decreases on cooling, which explains our experimental data in the low temperature region.

The interplay of paramagnetic and quadrupolar contributions yields T_1(T) dependence observed in the experiment.

Summary on VO_xNTs

Our NMR study of the multiwall vanadium oxide - decylamine nanotubes reveals diamagnetic V^{5+} and two paramagnetic V^{4+} ions, respectively. The amount of the V^{4+} ions was estimated as ~32% from the line intensities of the NMR spectra.

^{51}V spin-lattice relaxation data comprise both magnetic and quadrupolar contributions.

Collaboration :

Crystal growth and characterization:

C. C. Tang, *National Institute for Materials Science, Tsukuba, Japan*

R. Rosentsveig and R. Tenne, *Weizmann Institute for Science, Rehovot, Israel*

Cheol Eui Lee, *Department of Physics and Institute for Nano Science, Korea University, Seoul, Korea*

C. L. Teske and W. Bensch, *Christian-Albrechts University, Kiel, Germany*


"In the Negev will the talents of Jewish science and research be tested..." David Ben-Gurion

Thankyou!

Semimetal-semiconductor transformation on reduced size due to quantum confinement

Metal particle: quantum confinement is observed when the size is reduced to a value corresponding to the de Broglie wavelength; the density of states in the valence and conduction bands decreases, causing metal-nonmetal transition. Metals: de Broglie wavelength of the carriers is of the order of the lattice spacing. Thus quantum confinement is visible only for very small particles.

Semimetals and semiconductors: de Broglie wavelength may exceed the lattice spacing by several orders of magnitude, thus quantum confinement may be observed for rather large nanoparticles, i.e. for Tl_2Se nanorods with diameter of 75 nm and length of 900 nm.

Another example: semimetal Bi exhibits quantum confinement effects at a film thickness of ~100 nm. Bi nanowires show semimetal-semiconductor transition as the wire diameter is reduced down to 250 nm (Dresselhaus et al, Farhangfar).

Semiconductors show an increased band gap with reduction of size due to quantum mechanical effects.

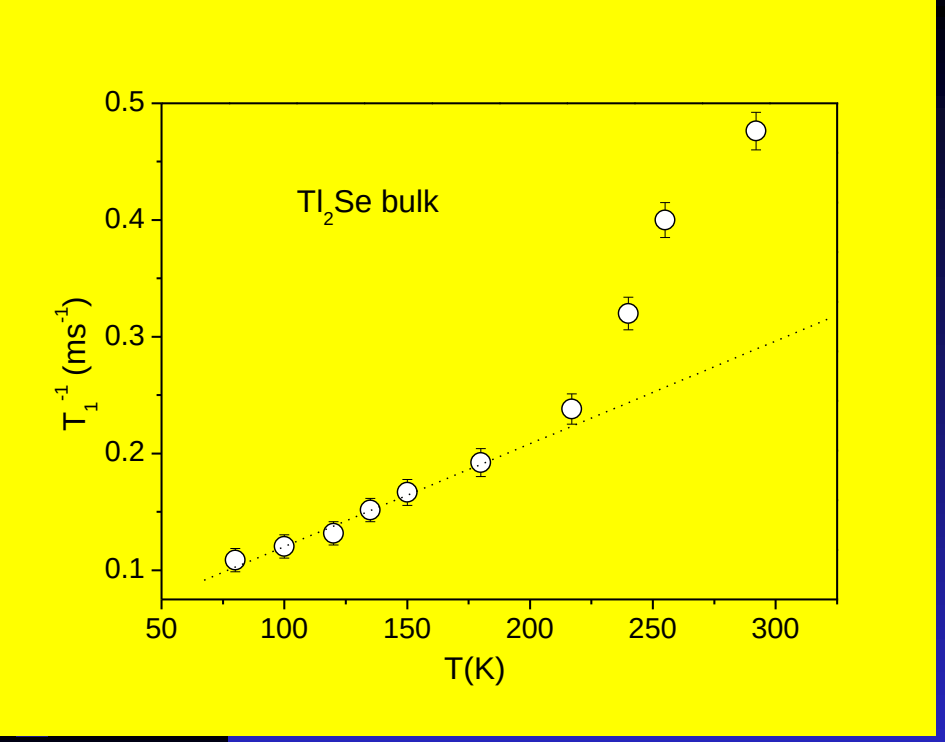

Temperature dependence of ^{205}Tl spin-lattice relaxation rate of Tl_2Se bulk sample in B_0=8.0196 T. Linear fit at low temperatures is shown by dotted line.

Metals: Korringa relation that arises from the interaction of nuclear spins with conduction electrons

$$\frac{1}{T_1T} = \frac{4\pi k}{\hbar}\left(\frac{\gamma_n}{\gamma_e}\right)^2 K^2 = const$$

In bulk Tl_2Se, the Korringa-like spin-lattice relaxation behavior is observed at low temperatures and is transformed to an activation regime above ~200 K. Interpretation: two-band model in the semimetallic compound, in which one band touches the Fermi level, while the second band is separated from the Fermi level by an energy gap ΔE. In this case, the relaxation rate is given by the expression

$$\frac{1}{T_1} = \frac{1}{T_{1K}} + CT\exp\left(-\frac{\Delta E}{2k_BT}\right)$$

ΔE = 0.16 eV.

Normally, the spin contribution to $1/T_{1K}T$ is proportional to the DOS at the Fermi-level. From linear fit of the data below 200 K, we obtained $1/T_{1K}T$ = 1.2 $s^{-1}K^{-1}$, that is much smaller than that of Tl metal, $1/T_1T \approx 330$ $s^{-1}K^{-1}$. The obtained value of $1/T_1T$ indicates much smaller DOS at the Fermi level of Tl_2Se in comparison with that in metallic thallium; such value is characteristic of semimetals.